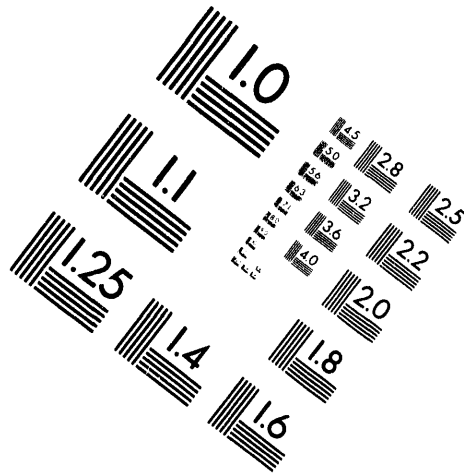
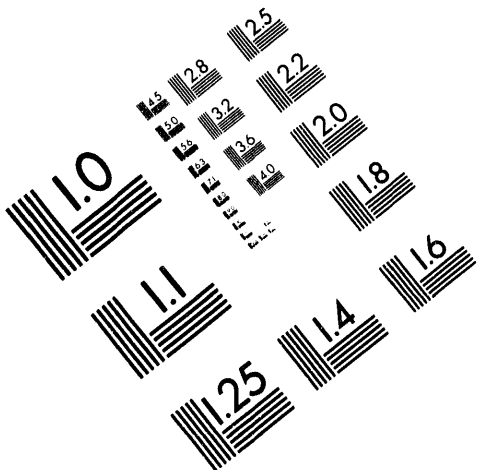




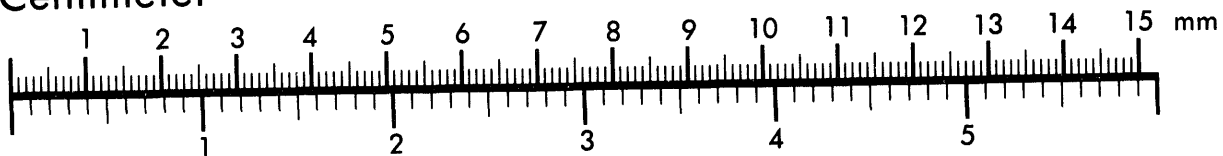
AIM

Association for Information and Image Management

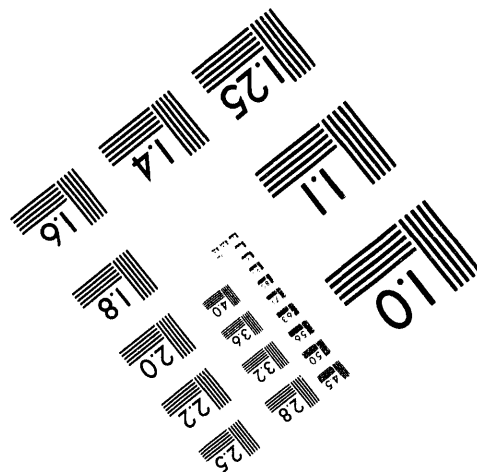
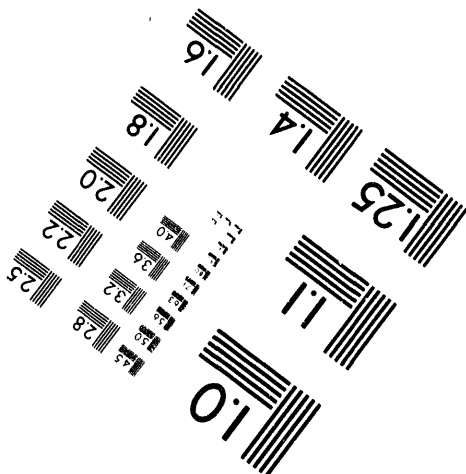
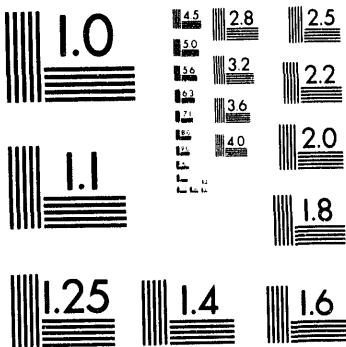
1100 Wayne Avenue, Suite 1100
Silver Spring, Maryland 20910
301/587-8202



Centimeter



Inches



MANUFACTURED TO AIM STANDARDS
BY APPLIED IMAGE, INC.

1 of 1

**Electron Heating and Current Drive by Mode Converted Slow
Waves.**

R. Majeski , C. K. Phillips, and J. R. Wilson

*Princeton Plasma Physics Laboratory, P.O. Box 451, Princeton, New Jersey
08543*

ABSTRACT

An approach to obtaining efficient single pass mode conversion at high parallel wavenumber from the fast magnetosonic wave to the slow ion Bernstein wave, in a two ion species tokamak plasma, is described. The intent is to produce localized electron heating or current drive via the mode converted slow wave. In particular, this technique can be adapted to off-axis current drive for current profile control. Modelling for the case of deuterium-tritium plasmas in TFTR is presented.

PACS numbers: 52.50.Gj, 52.55.Fa

MASTER

Introduction.

Mode conversion from the fast magnetosonic wave to the slow ion Bernstein wave (IBW) in a two-ion component plasma is known to play a part in ICRF (Ion Cyclotron Range of Frequency) heating schemes in tokamak plasmas. For example, mode conversion is predicted to be an important process in deuterium-tritium (D-T) plasmas,¹ where the densities of the two ion species are approximately equal. In experiments with a fast wave antenna on the high field side of the torus, IBW heating of electrons dominated the power flow.² Mode conversion and the modification of the fast wave polarization near the ion-ion hybrid resonance is known to be important in minority ion heating, especially at low parallel wavenumber (k_{\parallel}).^{1,3,4,5,6,7} Mode conversion from the fast wave to the slow Alfvén wave near the high field side plasma edge can be significant in large tokamaks.⁸

Most of the current generation of large tokamaks have high power long pulse ICRF systems for heating, with antennas sited on the low field side of the torus. Here we discuss a regime for efficient fast wave - IBW mode conversion in a two ion species plasma, for the purpose of direct electron heating or current drive by the IBW using existing low field side ICRF systems. For near-equal ion concentrations the mode conversion surface can be sited in the plasma core, while the ion cyclotron resonances are off axis in the colder regions of the plasma. This geometry limits fast wave ion heating. Efficient mode conversion is predicted at high k_{\parallel} for the proper choice of plasma parameters, so that the Bernstein wave phase velocity $v_{\phi}=\omega/k_{\parallel}$ is on the order of or less than the electron thermal velocity v_{Te} . Strong, localized electron damping of the Bernstein wave is expected to result.

An examination of the cold plasma resonance and cutoff surfaces shows that for parameters typical of large present-day tokamaks, these surfaces coalesce into a closely spaced cutoff-resonance-cutoff triplet at some experimentally accessible $k_{\parallel} \equiv k_{\parallel c}$. The evanescent layer between the low field side cutoff and the mode conversion surface is therefore thin for parallel wavenumbers slightly less than $k_{\parallel c}$, which enhances tunnelling of the fast wave from the low field side and the mode conversion efficiency. The presence of the second cutoff on the high field side of the resonance augments the wave electric field at the mode conversion surface to further increase the mode conversion efficiency. Such effects have been discussed for the Alfvén resonance^{4,8,9} but the importance of the high field side resonance in mode conversion at the ion-ion hybrid resonance has not been previously noted. Here we model for the first time the effect of a resonance-cutoff-resonance triplet on mode conversion in the experimentally important ion-ion hybrid case. Numerical results indicate that in excess of 80% per pass of the fast wave power incident on the triplet can be mode converted and coupled directly to electrons.

Efficient, off-axis heating of thermal electrons has potential applications in MHD control, current profile control, and electron heat transport studies. Off axis current drive is also of interest. Electron cyclotron heating could in principle provide a (proven) alternate bulk electron heating and current drive technique, but there are at present no microwave sources capable of supplying multimewatt long pulse power at appropriate frequencies. In contrast, all of the present generation of large tokamaks have high power heating systems in the ICRF. High efficiency mode conversion therefore has the potential for wide utilization in the near term in fusion research.

Cold plasma considerations.

For the ICRF the relevant cold plasma dispersion relation may be written:⁴

$$n_{\perp}^2 = \frac{(K_{\perp} + K_x - n_{\parallel}^2)(K_{\perp} - K_x - n_{\parallel}^2)}{(K_{\perp} - n_{\parallel}^2)} = \frac{(R - n_{\parallel}^2)(L - n_{\parallel}^2)}{(S - n_{\parallel}^2)} \quad (1)$$

where

$$K_{\perp} = 1 - \sum_j \frac{\omega_{pj}^2}{\omega^2 - \Omega_j^2}, \quad K_x = \sum_j \frac{\Omega_j}{\omega} \frac{\omega_{pj}^2}{\omega^2 - \Omega_j^2},$$

and $n_{\perp} = ck_{\perp}/\omega$, $n_{\parallel} = ck_{\parallel}/\omega$, $\omega_{pj}^2 = nq_j^2/(m_j \epsilon_0)$, $\Omega_j = q_j B_0/m_j$; m_j and q_j being the mass and charge of the j th species. The notation R, L, and S follows Stix.⁴ Mode conversion between the fast and slow modes occurs at the $n_{\parallel}^2 = S$ surface when hot plasma effects are included.¹ For a single ion species plasma, this surface occurs only for $\omega < \Omega_i$, and is referred to as the Alfvén resonance. For a plasma with two ion species an additional mode conversion surface appears at a frequency intermediate to the two ion cyclotron frequencies, and is referred to as the ion-ion hybrid resonance.

For the case of the ion-ion hybrid resonance in the situation usually considered, where k_{\parallel} is small and the fast wave is incident from the low field side, the fast wave is cutoff at the $n_{\parallel}^2 = L$ surface before reaching the resonance. Here the $n_{\parallel}^2 = R$ cutoff surface occurs at low density far from the resonance, and so the L and S surfaces form an isolated cutoff-resonance pair. In this case the

mode converted power can be shown to be given by $|T|^2(1-|T|^2)$, where $|T|=e^{-\eta}$ and η is the tunnelling factor.^{5,6,10}

We consider here a two-ion hybrid resonance regime where the $n_{||}^2=L$, R, and S surfaces occur in a closely spaced cutoff-resonance-cutoff triplet. Such a situation can be produced in present day large tokamaks in D-T plasmas by correctly choosing the species fraction, normalized frequency, and central density. We take TFTR as an example system. In Figure 1 a map of the locations in the equatorial plane of the cold plasma cutoffs and resonances for TFTR as a function of the parallel wavenumber are shown. The density profile was modelled as $n_e(r) \sim n_e(0)(1-(r/a)^{1.5})^{1.5}$, appropriate to a supershot discharge, with $n_e(0)=5 \times 10^{19} \text{ m}^{-3}$, major radius 2.62 m, minor radius 0.98 m, and a central toroidal field of 4.8 T. The assumed fractional concentration of tritium was $\eta_T \equiv n_T/n_e = 0.4$ in a deuterium plasma and the frequency, 33 MHz. The cutoffs and resonances coalesce at $R(\text{major radius}) \sim 2.3 \text{ m}$, or $r/a \sim 0.3$, for $k_{||} = k_{||c} \sim 12 \text{ m}^{-1}$. This wavenumber corresponds approximately to the peak in the vacuum antenna spectrum for the TFTR ICRH antennas, for 90° phasing, when toroidicity ($k_{||} \sim 1/R$) is included. For $k_{||} < k_{||c}$ the ordering of the cutoffs and resonances is the same as for the familiar minority ion heating regime; for $k_{||} > k_{||c}$ the ordering is the same as for the Alfvén regime^{4,8}. For $k_{||} = k_{||c}$ a cutoff is produced. In practice, $k_{||} < k_{||c}$ is required for good antenna coupling at the low field side edge. Two factors favor efficient mode conversion for $k_{||}$ on the order of (but less than) $k_{||c}$: the proximity of the $n_{||}^2=L$ cutoff and the $n_{||}^2=S$ resonance which allows efficient tunnelling through the evanescent layer, and the second cutoff at $n_{||}^2=R$ which reflects transmitted fast wave power back into the resonance from the high field side.

The resonance location is primarily determined by the frequency and the relative concentration of the two ion species (deuterium and tritium here), and

so off-axis electron heating and current drive is possible. In fast wave direct electron heating and current drive, by contrast, the inverse damping length of the fast wave on electrons $\text{Im}(k_{\perp})$ scales as $\text{Re}(k_{\perp})\beta_e\xi e^{-\xi^2}$, where β_e is the electron beta and $\xi = \omega/k_{\parallel}v_{Te}$.¹¹ The linear dependence of the inverse damping length on $\beta_e \sim n_e T_e$ produces a power deposition profile which is always peaked on axis.

In the mode conversion case, the radial location of the power deposition can be varied with the frequency. In the limit where $n_{\parallel}^2 \gg 1$ but $\omega_{pi}^2 \gg n_{\parallel}^2 \omega^2$ the location of the resonance in major radius may be approximated as

$$R = \frac{1}{\omega} \frac{eB_0 R_0}{m_1} \left[\frac{\omega_{p2}^2 + \omega_{p1}^2 \mu_{rel}^2}{\omega_{p1}^2 + \omega_{p2}^2} \right]^{1/2} \quad (2)$$

where R_0 is the major radius of the axis, B_0 is the on-axis toroidal field, and μ_{rel} is ratio of the ion masses. Since $R \sim 1/\omega$ here, a 10% variation in the frequency of the coupled fast wave would be sufficient to vary the location of the resonance, and the resulting slow wave heating or current drive, by $\Delta r/a \sim 0.25$ for typical tokamak aspect ratios. Active profile control in future long-pulse tokamaks may therefore be possible.

Mode conversion efficiency

In the absence of the secondary high field side cutoff, the mode conversion efficiency is determined by the tunnelling factor, which can be approximated in plane geometry as^{7,8}

$$\eta = \frac{-(\pi/2)(D_0^2/S')}{(-(D^2)'/S')^{1/2}} \quad (3)$$

Here $D=1/2(R-L)$ and the subscript 0 denotes evaluation at the spatial position of the $n_{\parallel}^2=S$ resonance. S and D^2 have been linearized in the spatial coordinate x as $S-n_{\parallel}^2=S'x$ and $D^2=D_0^2+(D^2)'x$, where x , y , and z respectively denote the radial, poloidal, and toroidal directions and are normalized to c/ω .

In Fig. 2 we plot the estimate of the percentage of the mode converted power $|T|^2(1-|T|^2)$, $|T|=e^{-\eta}$, as a function of k_{\parallel} using Eq. (3) to determine η . Plasma parameters were the same as for Fig. 1. Also shown in Fig. 2 is an estimate of the mode converted power using the fourth order 1-D full wave code CARDS.¹² Here the spatial extent of the plasma slab modelled included the $n_{\parallel}^2=L$ cutoff and $n_{\parallel}^2=S$ resonance only; the high field side $n_{\parallel}^2=R$ cutoff was excluded. Competing absorption mechanisms are not considered. The numerical modelling assumed a central ion temperature $T_i(0)=20$ keV, and a central electron temperature $T_e(0)=10$ keV, with a profile varying as $T_{i,e}(0)(1-(r/a)^{1.5})^{2.5}$ appropriate to a supershot discharge in TFTR. For this case the analytic expression for the mode converted power and the numerical results are in excellent agreement. Both indicate that, for the isolated cutoff-resonance case there is a broad maximum in the mode conversion efficiency at $k_{\parallel} = 8 - 10$ m^{-1} ; or somewhat below $k_{\parallel c}$.

For the case of interest here, which includes the $n_{\parallel}^2=R$ cutoff, it has been shown that the mode converted power can in general be written as

$$P_c = \pi \frac{D_0^2}{S'} |E_y|^2, \quad (4)$$

where $|E_y|$ is the y (poloidal) component of the electric field at the resonance.⁸ The presence of a nearby cutoff would be expected to modify the mode conversion efficiency by modifying $|E_y|$ at the resonance. This effect has not

previously been included in estimates of mode conversion efficiency. Note that, unlike the case of a nearby conducting wall,⁸ $|E_y|$ does not vanish at the cutoff. The result of numerical modelling with the CARDS code in which the high field side $n_{||}^2=R$ cutoff is included is also shown in Fig. 2. For high $k_{||}$ (9-11.5 m^{-1}) the mode conversion efficiency is predicted to be significantly increased by the inclusion of the high field side cutoff. For this range in wavenumber the distance between the $n_{||}^2=R$ cutoff and the mode conversion layer is less than half the radial wavelength of the transmitted fast wave, where the proximity of the cutoff significantly increases the wavelength. The increase in the mode conversion efficiency is found to scale as $|E_y^c|^2 / |E_y|^2$, where $|E_y^c| (|E_y|)$ is numerically determined with (without) the high field side cutoff. The effect of a standing-wave pattern in $|E_y|$ due to reflection at the high field side cutoff is further evidenced by the elimination of mode conversion for $k_{||}=8.5 m^{-1}$. This value of the wavenumber is associated with a null in $|E_y|$ at the $n_{||}^2=S$ resonance. The full width at half maximum (FWHM) of the region in parallel wavenumber where enhanced mode conversion is obtained is larger than the FWHM of the TFTR ICRF antenna spectrum (the two-strap TFTR antennas are not optimized for current drive), but is of the same order as the predicted spectral width of antennas designed for fast wave current drive.¹³ Note that numerical modelling with the inclusion of the high field side cutoff for $k_{||}<6.75 m^{-1}$ could not be performed due to the proximity of the tritium cyclotron resonance. Modelling with the sixth order full-wave 1-D code FELICE¹⁴ shows similar high mode conversion efficiency for these parameters.

The power deposition profile calculated using CARDS for the case discussed in relation to Figures (1) and (2) is shown in Fig. 3, where the full cutoff-resonance-cutoff is now modelled. A wavenumber of $k_{||}=10 m^{-1}$ is assumed. Here the code boundaries include the fundamental ion cyclotron

resonance of deuterium 10 cm to the low field side of the axis. Since deuterium is in effect the majority species here, there is only 10% single-pass absorption of the incident fast wave on the deuterium, despite the 20 keV ion temperature. 20% of the incident power is reflected, with the remainder (70%) undergoing mode conversion and absorption on the electrons at $r/a \sim 0.4$ on the high-field side of the axis. The radial location of power deposition is a few cm to the high field side of the $n_{||}^2=S$ resonance. The full width at half maximum (FWHM) of the power deposition profile is 6 cm. For this parameter regime, direct single pass absorption of the fast wave (which peaks near $x=0$) by electrons is negligible in comparison to the mode converted power.

Since the absorbed wave is a slow mode, single-pass absorption efficiency is less dependent on the electron temperature than in the case of direct electron heating by fast waves. Numerical results with variations of the central electron temperature from 2 to 30 keV, while keeping all other parameters constant, indicate that the mode converted power flow to electrons varies by less than 5% over this range in T_e . The power deposition profile does, however, broaden as T_e is reduced, from a FWHM value of 5 cm at $T_e(0)=30$ keV to 20 cm at 2 keV. Direct electron damping of the fast wave, by contrast, is negligible at 2 keV and is predicted to increase to only 4% per pass at 30 keV.

The increase in mode conversion efficiency which results from the presence of the secondary high field side cutoff is further demonstrated in Fig. 4. Figure 4 is a plot of the numerically estimated absorbed, reflected, and transmitted wave power, using CARDS, as a function of the position of the high field side boundary. The low field side (source) boundary is located at $R=3.0$ m, the $n_{||}^2=L$ cutoff and adjacent $n_{||}^2=S$ resonance are located at $R=2.35$ m, and the $n_{||}^2=R$ cutoff is located at $R=2.15$ m. As the absorbing boundary is moved through the $n_{||}^2=L$ and S surfaces the reflected power increases to

approximately 25%, and a similar fraction of the power is mode converted and coupled to the electrons. As the $n_{||}^2=R$ cutoff is traversed the transmitted power drops to zero while the mode converted power absorbed on electrons increases due to the fast wave reflection from the cutoff and the resultant increased electric field at the mode conversion surface. The high mode conversion efficiency predicted by numerical modelling with the CARDS code is due to inclusion of the full resonance-cutoff-resonance triplet in the modelling region.

Current drive efficiency

For plasma parameters of interest in near-term large tokamaks the coalescence of the cutoff and resonant surfaces will occur at relatively large $k_{||}$, and hence low v_{ϕ} . For the example TFTR case discussed in conjunction with Fig. 3, $v_{\phi}/v_{Te} \sim 0.5$ in the region where power is deposited on electrons, at $r/a=0.3-0.4$ on the high field side of the axis. It has been shown that for power deposition on the high field side of the axis the reduction of current drive efficiency due to trapped electron effects is minimized.¹⁵ We estimate the driven current for the example case using the Ehst-Karney parameterization¹⁵ for the current drive efficiency. All power is assumed to be deposited at an inverse aspect ratio $\epsilon=0.1$. Since the single pass absorption is high, 90% of the launched fast wave power will be deposited on electrons in a few passes. For a Z_{eff} of 2, therefore, the driven current is estimated to be 0.07 A/W of coupled fast wave power. Here Landau damping of the IBW is assumed to dominate. The figure of merit for current drive efficiency $\gamma \equiv (\bar{n}_e R_T / 10^{20})(I/P_{rf}) = 0.06 \text{ A-W}^{-1} \text{ m}^{-2}$.

Studies have shown that for high parallel phase velocity waves ($N_{||} \equiv ck_{||}/\omega = 0.1$) the magnitude and sign of the Bernstein parallel wavenumber change as the wave propagates when poloidal field effects are included.¹⁶

Without resorting to a fully toroidal hot plasma treatment, we can estimate the change in k_{\parallel} due to poloidal field effects before the Bernstein wave is damped in our low phase velocity ($N_{\parallel}=11$) case using the 1-D code CARDS. At the mode conversion surface, the Bernstein wave vector lies in the direction of decreasing major radius ($\mathbf{k} \approx -\mathbf{k}_x$, where x is in the major radial direction). For propagation exactly in the plasma midplane the parallel wavenumber is largely preserved.¹⁶ Above or below the midplane the parallel wavenumber will undergo an up- or down- shift, depending on the sense of the rotational transform. In a poloidal magnetic field, $k_{\parallel} = k_{\Theta}(B_{\Theta}/B) + n(B_{\Phi}/B)/(R + r \cos \Theta)$,¹⁶ where k_{Θ} denotes the projection of the Bernstein wavenumber onto the poloidal direction, B_{Θ} denotes the poloidal and B_{Φ} the toroidal field, and Θ is the poloidal angle. For the case considered here, numerical modelling indicates that 90% of the power in the Bernstein wave is damped with $k_x < 200 \text{ m}^{-1}$. The dispersion relation of the Bernstein wave was obtained using the CARDS code and is approximately valid, since $k_{\perp} \rho_i < 1$. Assuming that the mode conversion layer (at $r/a=0.4$) is located near the $q=2$ surface, then within $\pm 15 \text{ cm}$ vertical displacement from the midplane poloidal effects will cause less than a 50% change in the IBW parallel wave number before the wave is damped. Thus for mode conversion at low phase velocity (high k_{\parallel}), in a sufficiently dense plasma for good wave focussing to occur, poloidal effects are not expected to dominate.

Finally, we note that if the mode conversion layer, and therefore the peak in the power deposition profile, is located on-axis, then the absence of trapped particle effects would increase the projected current drive efficiency to $0.17 \text{ A} \cdot \text{W}^{-1}$, again for TFTR parameters. Operation at low v_{ϕ}/v_{Te} (high momentum input) can further increase the current drive efficiency in this case by an additional factor of ~ 2 .¹⁵ Down shifts of the parallel wavenumber due to

poloidal field effects may significantly modify the current drive efficiency in this case, however.

Conclusions

A regime for efficient excitation of the ion Bernstein wave via mode conversion of the fast magnetosonic wave for values of the launched wavenumber somewhat less than $k_{\parallel c}$, where $k_{\parallel c}$ denotes the wavenumber at which the $n_{\parallel}^2=L$, R and S surfaces coalesce, is discussed. This regime is a suitable candidate for on- or off-axis direct heating of electrons, and on- or off-axis current drive, to provide current profile control in the present generation of large tokamaks, using existing ICRF systems. Numerical modelling based on a deuterium-tritium ion system in TFTR indicates that single-pass absorption on electrons of 70% can be obtained in this regime with narrow (<10 cm) power deposition profiles. By contrast, single-pass direct electron absorption on the fast wave for the same plasma parameters is indicated to be weak (<5%). The mode converted Bernstein wave is damped on thermal electrons, with $\nu_{\phi} \sim \nu_{Te}$. Trapped electron effects are minimized by localizing the power deposition to the high field side of the magnetic axis, however. Predicted off-axis current drive efficiency is approximately 0.07 AW^{-1} for typical TFTR parameters.

Acknowledgments

The authors acknowledge many useful conversations and comparisons of numerical results with E. F. Jaeger. CARDS was developed by D. Smithe, while the FELICE code was developed by M. Brambilla. Indispensable instruction in the operation of FELICE, as well as other valuable advice, was

obtained from P. Bonoli, A. Bers, R. Hawryluk, J. Hosea, and M. Murakami all provided useful insight. This work was supported by U. S. Department of Energy Contract DE-AC02-76-CHO-3073.

References

1. F. W. Perkins, Nucl. Fusion 17, 1197 (1977).
2. Equipe TFR, in *Plasma physics and Controlled Nuclear Fusion Research 1982*, Proc. 9th Conference, Baltimore, 1982 (IAEA, Vienna, 1983) Vol. II, p. 17.
3. M. Brambilla and T. Krucken, Nucl. Fusion 28, 1813 (1988).
4. T. H. Stix, *Waves in Plasmas*, American Institute of Physics, New York (1992).
5. D. G. Swanson, Phys. Fluids 28, 2645 (1985).
6. V. Fuchs and A. Bers, Phys. Fluids 31, 3702 (1988).
7. J. Jacquinet, B. D. McVey, and J. E. Scharer, Phys. Rev. Lett. 39, 88 (1977).
8. J. A. Heikkinen, T. Hellsten, M. J. Alava, Nucl. Fusion 31, 417 (1991).
9. C. F. F. Karney, F. W. Perkins, and Y. -C. Sun, Phys. Rev. Lett. 42, 1621 (1979).
10. M. J. Alava and J. A. Heikkinen, Physica Scripta 45, 345 (1992).

11. M. Porkolab, in *Radio Frequency Power in Plasmas, Proceedings, Ninth Topical Conference, Charleston, 1991* (American Institute of Physics Conference Proceedings 244, New York, 1991) p. 197.

12. D. N. Smithe, Ph.D. thesis, University of Michigan, 1987.

13. D. W. Swain, et al., in *Radio Frequency Power in Plasmas, Proceedings Tenth Topical Conference, Boston, 1993* (American Institute of Physics Conference Proceedings 289, New York, 1994) p. 371.

14. M. Brambilla, *Nucl. Fusion* 28, 549 (1988).

15. D. A. Ehst and C. F. F. Karney, *Nucl Fusion* 31, 1933 (1991).

16. A. K. Ram and A. Bers, *Phys. Fluids B* 3, 1059 (1991).

Figure Captions.

Figure 1. Map of the cold plasma cutoff and resonant surfaces in k_{\parallel} and major radius for TFTR. L denotes the $n_{\parallel}^2=L$ cutoff, S denotes the $n_{\parallel}^2=S$ resonance, and R denotes the $n_{\parallel}^2=R$ low density cutoff. The locations of the fundamental cyclotron resonances of deuterium and tritium are indicated by Ω_D and Ω_T .

Figure 2. Estimates of the percentage of the incident power which is mode converted. The solid line denotes the analytic estimate obtained using Eq. 3 to determine η for the isolated cutoff-resonance case. The crosses indicate the numerical results obtained with the 1-D code CARDS for the same case. The triangles indicate the numerical results for the mode converted power fraction when the additional high field side cutoff is included.

Figure 3. Power deposition profiles computed with CARDS. Electron absorption is indicated by E, deuterium absorption by D, and tritium absorption (which is negligible throughout the modelled region) by T. The plasma axis is at 2.62 m.

Figure 4. Absorbed, reflected, and transmitted power as a function of the spatial position of the high field side boundary of the modelled region. Here E denotes power absorbed on electrons, D indicates deuterium absorption, R indicates reflected power, and T denotes the power transmitted to the boundary.

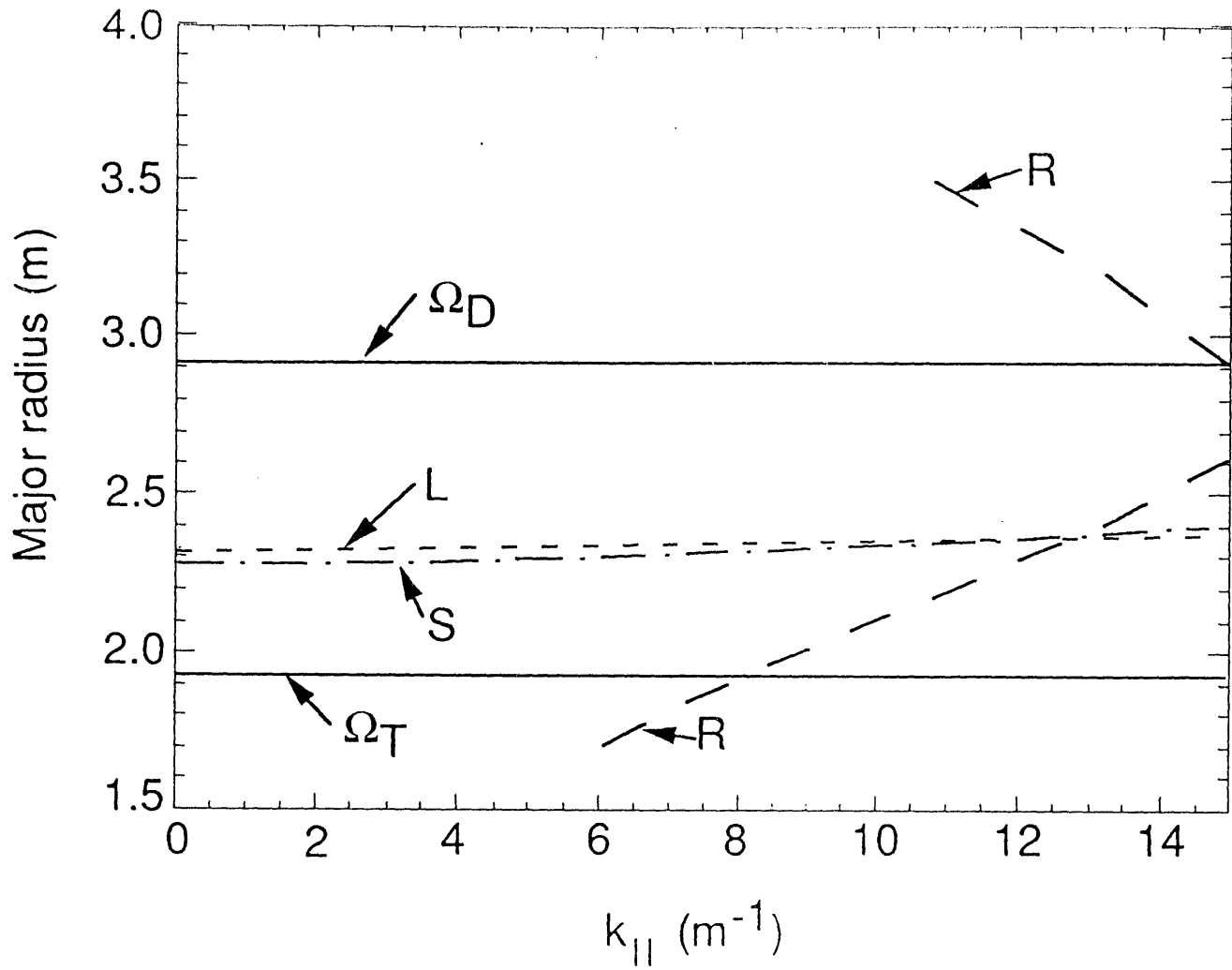


Figure 1

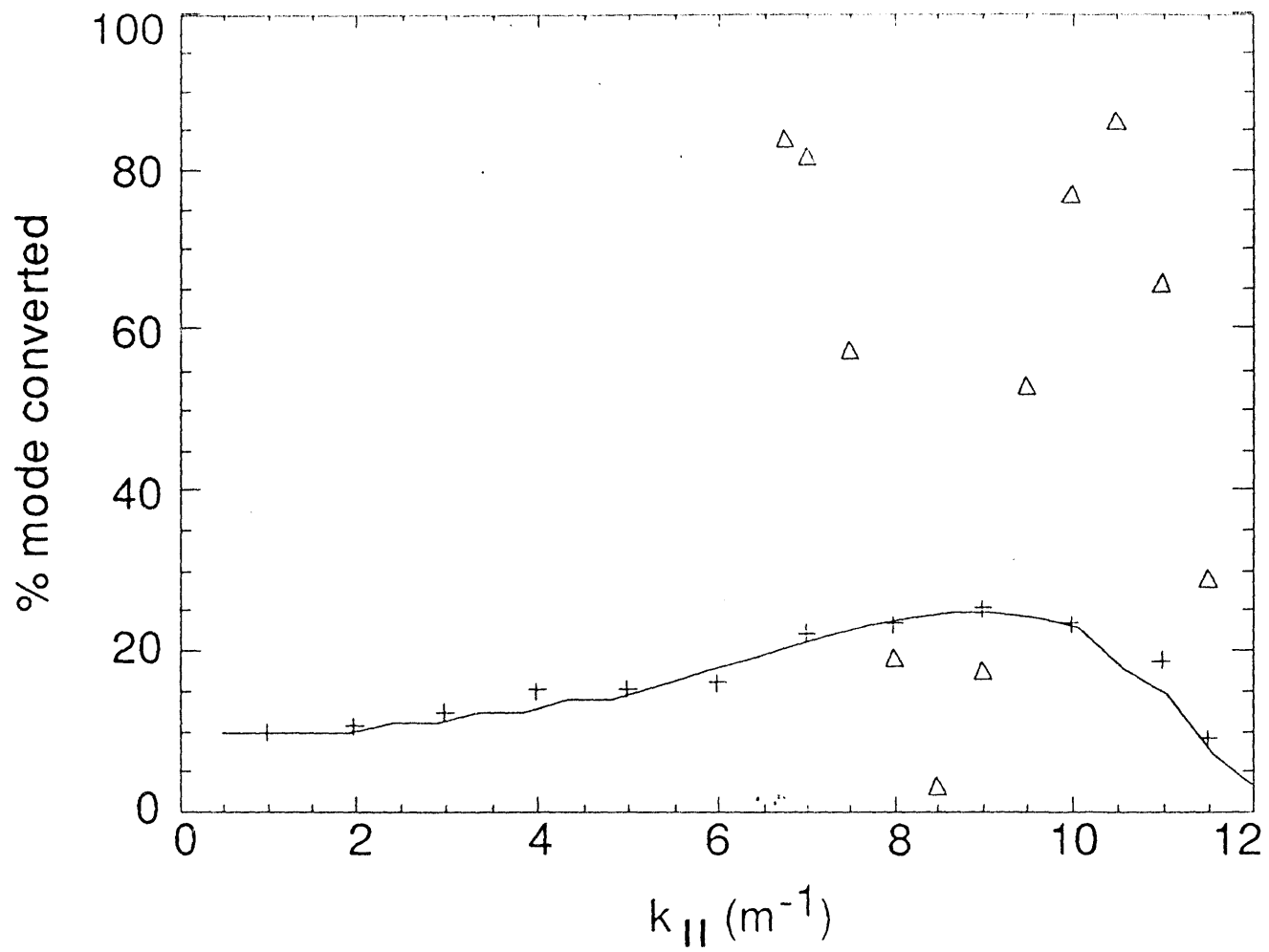


Figure 2

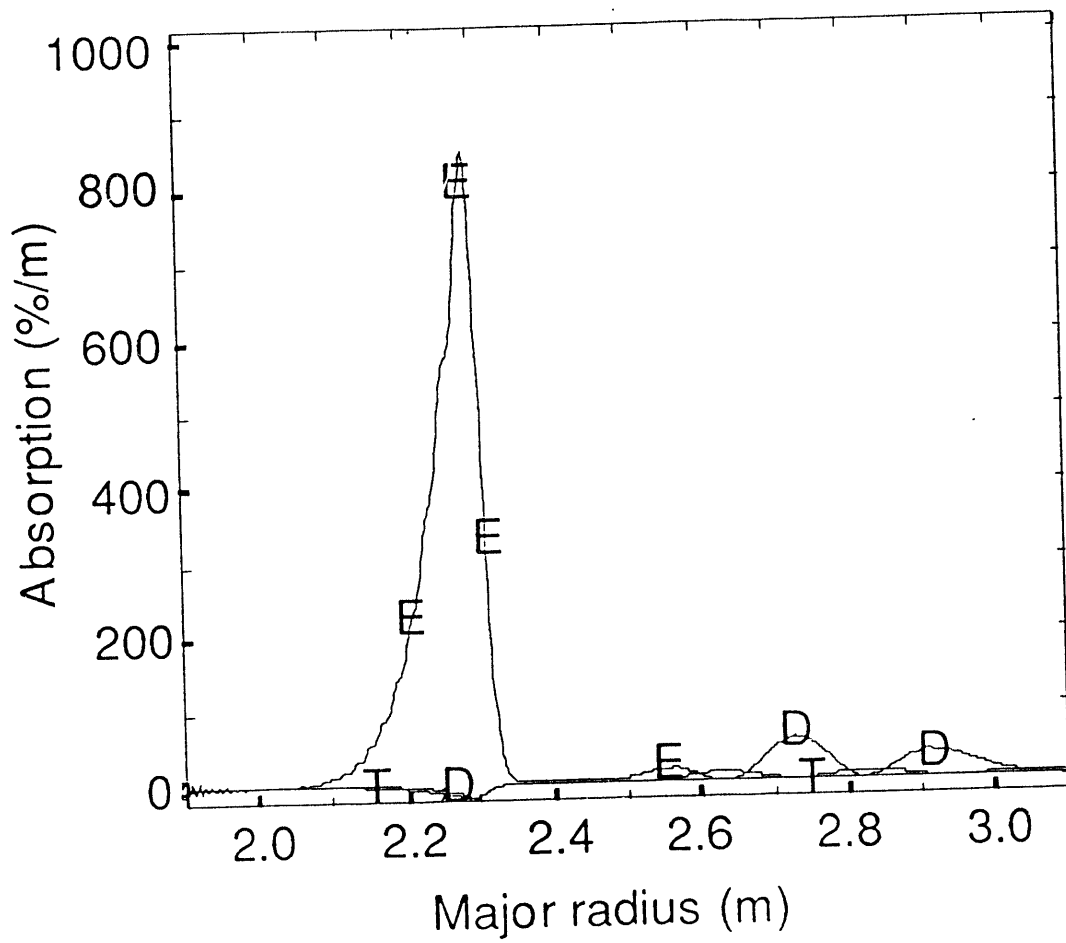
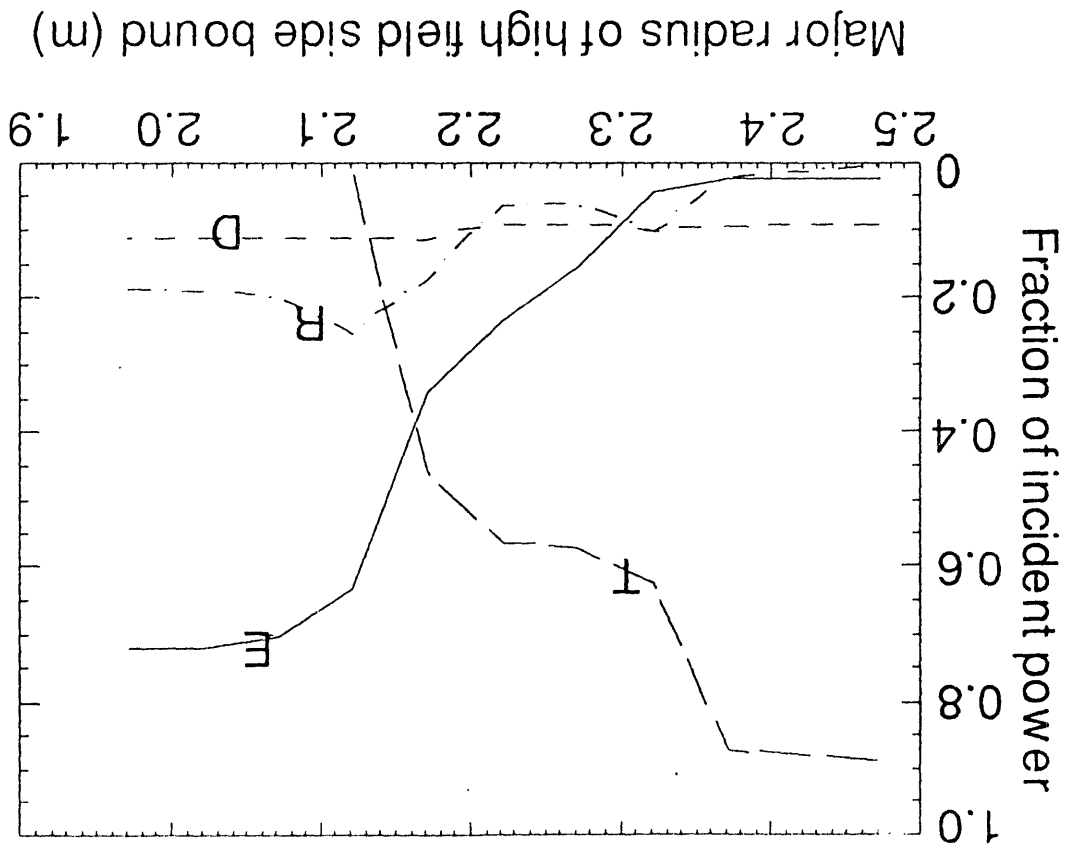


Figure 3

Figure 4



EXTERNAL DISTRIBUTION IN ADDITION TO UC-420

Dr. F. Paoloni, Univ. of Wollongong, AUSTRALIA
 Prof. R.C. Cross, Univ. of Sydney, AUSTRALIA
 Plasma Research Lab., Australian Nat. Univ., AUSTRALIA
 Prof. I.R. Jones, Flinders Univ, AUSTRALIA
 Prof. F. Cap, Inst. for Theoretical Physics, AUSTRIA
 Prof. M. Heindler, Institut für Theoretische Physik, AUSTRIA
 Prof. M. Goossens, Astronomisch Instituut, BELGIUM
 Ecole Royale Militaire, Lab. de Phy. Plasmas, BELGIUM
 Commission-European, DG. XII-Fusion Prog., BELGIUM
 Prof. R. Bouciqué, Rijksuniversiteit Gent, BELGIUM
 Dr. P.H. Sakanaka, Instituto Fisica, BRAZIL
 Prof. Dr. I.C. Nascimento, Instituto Fisica, Sao Paulo, BRAZIL
 Instituto Nacional De Pesquisas Espaciais-INPE, BRAZIL
 Documents Office, Atomic Energy of Canada Ltd., CANADA
 Ms. M. Morin, CCFM/Tokamak de Varennes, CANADA
 Dr. M.P. Bachynski, MPB Technologies, Inc., CANADA
 Dr. H.M. Skarsgard, Univ. of Saskatchewan, CANADA
 Prof. J. Teichmann, Univ. of Montreal, CANADA
 Prof. S.R. Sreenivasan, Univ. of Calgary, CANADA
 Prof. T.W. Johnston, INRS-Energie, CANADA
 Dr. R. Bolton, Centre canadien de fusion magnétique, CANADA
 Dr. C.R. James,, Univ. of Alberta, CANADA
 Dr. P. Lukác, Komenského Univerzita, CZECHO-SLOVAKIA
 The Librarian, Culham Laboratory, ENGLAND
 Library, R61, Rutherford Appleton Laboratory, ENGLAND
 Mrs. S.A. Hutchinson, JET Library, ENGLAND
 Dr. S.C. Sharma, Univ. of South Pacific, FIJI ISLANDS
 P. Mähönen, Univ. of Helsinki, FINLAND
 Prof. M.N. Bussac, Ecole Polytechnique,, FRANCE
 C. Mouttet, Lab. de Physique des Milieux Ionisés, FRANCE
 J. Radet, CEN/CADARACHE - Bat 506, FRANCE
 Prof. E. Economou, Univ. of Crete, GREECE
 Ms. C. Rinni, Univ. of Ioannina, GREECE
 Preprint Library, Hungarian Academy of Sci., HUNGARY
 Dr. B. DasGupta, Saha Inst. of Nuclear Physics, INDIA
 Dr. P. Kaw, Inst. for Plasma Research, INDIA
 Dr. P. Rosenau, Israel Inst. of Technology, ISRAEL
 Librarian, International Center for Theo Physics, ITALY
 Miss C. De Palo, Associazione EURATOM-ENEA , ITALY
 Dr. G. Grosso, Istituto di Fisica del Plasma, ITALY
 Prof. G. Rostangni, Istituto Gas Ionizzati Del Cnr, ITALY
 Dr. H. Yamato, Toshiba Res & Devel Center, JAPAN
 Prof. I. Kawakami, Hiroshima Univ., JAPAN
 Prof. K. Nishikawa, Hiroshima Univ., JAPAN
 Librarian, Naka Fusion Research Establishment, JAERI, JAPAN
 Director, Japan Atomic Energy Research Inst., JAPAN
 Prof. S. Itoh, Kyushu Univ., JAPAN
 Research Info. Ctr., National Instit. for Fusion Science, JAPAN
 Prof. S. Tanaka, Kyoto Univ., JAPAN
 Library, Kyoto Univ., JAPAN
 Prof. N. Inoue, Univ. of Tokyo, JAPAN
 Secretary, Plasma Section, Electrotechnical Lab., JAPAN
 Dr. O. Mitarai, Kumamoto Inst. of Technology, JAPAN
 Dr. G.S. Lee, Korea Basic Sci. Ctr., KOREA
 J. Hyeon-Sook, Korea Atomic Energy Research Inst., KOREA
 D.I. Choi, The Korea Adv. Inst. of Sci. & Tech., KOREA
 Prof. B.S. Liley, Univ. of Waikato, NEW ZEALAND
 Inst of Physics, Chinese Acad Sci PEOPLE'S REP. OF CHINA
 Library, Inst. of Plasma Physics, PEOPLE'S REP. OF CHINA
 Tsinghua Univ. Library, PEOPLE'S REPUBLIC OF CHINA
 Z. Li, S.W. Inst Physics, PEOPLE'S REPUBLIC OF CHINA
 Prof. J.A.C. Cabral, Instituto Superior Tecnico, PORTUGAL
 Prof. M.A. Hellberg, Univ. of Natal, S. AFRICA
 Prof. D.E. Kim, Pohang Inst. of Sci. & Tech., SO. KOREA
 Prof. C.I.E.M.A.T, Fusion Division Library, SPAIN
 Dr. L. Stenflo, Univ. of UMEA, SWEDEN
 Library, Royal Inst. of Technology, SWEDEN
 Prof. H. Wilhelmson, Chalmers Univ. of Tech., SWEDEN
 Centre Phys. Des Plasmas, Ecole Polytech, SWITZERLAND
 Bibliotheek, Inst. Voor Plasma-Fysica, THE NETHERLANDS
 Asst. Prof. Dr. S. Cakir, Middle East Tech. Univ., TURKEY
 Dr. V.A. Glukhikh, Sci. Res. Inst. Electrophys. I Apparatus, USSR
 Dr. D.D. Ryutov, Siberian Branch of Academy of Sci., USSR
 Dr. G.A. Eliseev, I.V. Kurchatov Inst., USSR
 Librarian, The Ukr.SSR Academy of Sciences, USSR
 Dr. L.M. Kovrizhnykh, Inst. of General Physics, USSR
 Kernforschungsanlage GmbH, Zentralbibliothek, W. GERMANY
 Bibliothek, Inst. Für Plasmaforschung, W. GERMANY
 Prof. K. Schindler, Ruhr-Universität Bochum, W. GERMANY
 Dr. F. Wagner, (ASDEX), Max-Planck-Institut, W. GERMANY
 Librarian, Max-Planck-Institut, W. GERMANY

DATE

FILMED

10/13/94

END

